ISSN 0915-633X

NIFS—230

JP9311137

Transition of Radial Electric Field by Electron Cyclotron Heating in Stellarator Plasmas

H. Idei, K. Ida, H. Sanuki, H. Yamada, H. Iguchi, S. Kubo,
R. Akiyama, H. Arimoto, M. Fujiwara, M. Hosokawa,
K. Matsuoka, S. Morita, K. Nishimura, K. Ohkubo, S. Okamura,
S. Sakakibara, C. Takahashi, Y. Takita, K. Tsumori and I. Yamada

(Received – Mar. 1, 1993)

NIFS-230 June 1993

Transition of Radial Electric Field by Electron Cyclotron Heating in Stellarator Plasmas

H. Idei, K. Ida, H. Sanuki, H. Yamada, H. Iguchi, S. Kubo,

R. Akiyama, H. Arimoto,[a] M. Fujiwara, M. Hosokawa, K. Matsuoka,

S. Morita, K. Nishimura, K. Ohkubo, S. Okamura, S. Sakakibara,

C. Takahashi, Y. Takita, K. Tsumori and I. Yamada

National Institute for Fusion Science, Nagoya 464-01, Japan

(Received 1993)

Abstract

The transition of a radial electric field from a negative to a positive value is observed in Compact Helical System when the electron loss is sufficiently enhanced by the superposition of the off-axis second harmonic electron cyclotron heating on the neutral beam heated plasmas. The observed threshold for the enhanced particle flux required to cause the transition is compared with a theoretical prediction.

Keywords:

transition, radial electric field, density pump-out, electron cyclotron heating, stellarator, neoclassical particle flux,

A radial electric field near the plasma periphery has been found to play an important role on the improved confinement such as in the H-mode plasmas[1-3]. Theoretical models of the L/H transition in tokamaks have been proposed. It is predicted that the change in the radial electric field or in the plasma rotation has a strong influence on the transition[4-8]. In stellarator devices, the neoclassical theory suggests that the electric field reduces the helical ripple loss, and consequently improves the plasma confinement[9-11]. Multiple solutions of the electric field that satisfy the ambipolar constraint often arise when particle fluxes have a nonlinear dependence on the electric field. There are generally two stable states in the stellarator plasmas which are called the ion and the electron roots[11]. In a stellarator reactor, it is an important scenario to attain the electron root with higher energy confinement time through heating electrons in the startup phase[9]. In Heliotron-E device, the radial electric field at $r \simeq 0.7\text{-}0.9a$ is found to be positive (the electron root) for the low density plasma($n_e < 1 \times 10^{13}\text{cm}^{-3}$), and negative (the ion root) for the high density plasma($n_e > 2 \times 10^{13}\text{cm}^{-3}$)[12]. In Wendelstein VII-A stellarator, the observed electric field in the plasma with electron cyclotron heating(ECH) ($n_e \sim 5 \times 10^{13}$ cm^{-3}) is consistent with a theoretical prediction[13]. In Compact Helical System(CHS)[14], the observed radial electric field is negative in the typical neutral beam(NB) heated plasmas[15]. The electric field becomes more negative near the plasma edge for the higher electron density.

It is generally observed that ECH has an effect of density pump-out both in tokamaks[16] and stellarators[17,18]. In CHS, it is observed that the particle confinement becomes worse in the plasma with second harmonic ECH at low field side resonance than at high field side one[19]. One of the candidates to explain the mechanism of the density pump-out is the outward flux due to the poor confinement of perpendicularly accelerated electrons by ECH[20]. In this letter, we present the transition of the radial electric field from the ion root to the electron root triggered by enhancing the electron particle flux with ECH.

CHS is a heliotron/torsatron device with a pole number of an l=2, a toroidal period number m=8 and an aspect ratio of 5. The major radius R is 92cm and the averaged minor radius a is 19cm. The second harmonic ECH is carried out with the 53.2GHz gyrotron of the maximum pulse width of 100ms. Here, the more than 60 % of the injection power is focused into a beam with a 2.5cm 1/e spot size on the mid-plane of CHS vacuum vessel with a desired extraordinary mode. The focusing system is composed of a stair cut Vlasov antenna, an improved reflecting mirror, a reflecting corrugated polarizer and a steerable focusing mirror[18]. The 7.5MHz ion cyclotron range of frequency(ICRF) is used for the pre-ionization of plasmas in this study[21]. The neutral beam is tangentially injected to sustain the plasmas and to utilize a charge exchange spectroscopy(CXS). Poloidal rotation and ion temperature

are measured with CXS with a time resolution $\Delta t_{CXS} = 16.7$ms[22]. The radial electric field is evaluated from the observed poloidal rotation and the ion pressure gradient using a radial momentum balance equation for a fully ionized carbon. In the momentum balance equation, a toroidal rotation has a little contribution to the radial electric field, because the toroidal rotation damps due to a viscous damping force caused by the helical ripple[23].

The second harmonic ECH is superposed to an NB heated target plasma in order to enhance the electron particle flux. The density in the NB heated target plasma is controlled to stay below the cut-off density. The focus point of ECH is located at r=0.5a in the low field side region, since the enhanced electron flux at the low field side resonance heating is expected to be larger than at the high field side resonance heating. A line-averaged electron density decreases with the superposition of ECH. The enhanced electron flux is controlled by changing the ECH injection power(P_{ECH}=85,105 and 140kW). Figure 1 shows radial profiles of electron density $n_e(\rho)$ and temperature $T_e(\rho)$, measured with Thomson scattering(TS), ion temperature $T_i(\rho)$ and poloidal rotation velocity $v_\theta(\rho)$, measured with CXS at 15ms after the ECH is turned on for the plasmas with P_{ECH} = 85 and 140kW, where ρ is a normalized radius calculated with finite β equibrium code, VMEC[24]. The experiments for the plasmas with P_{ECH}=85, 105 and 140kW are carried out for the target plasma with a fixed density(~9.5 ×

10^{12}cm^{-3}). As a reference plasma, we choose the plasma such that the line-averaged density is adjusted to be as low as that for the plasma with $P_{\rm ECH}$=140kW to eliminate the density dependence of the radial electric field. Radial profiles $n_e(\rho)$, $T_e(\rho)$, $T_i(\rho)$ and $v_\theta(\rho)$ for the reference plasma, and $n_e(\rho)$ for the target plasma are also shown in Fig.1. The plasmas with $P_{\rm ECH}$=105 and 140kW rotate in the ion-diamagnetic direction which means the positive electric field, while the small rotation velocity is observed for the target plasma, the reference plasma and that with $P_{\rm ECH}$=85kW.

Figure 2 (a) shows time evolutions of the line-averaged densities for the target plasma $\bar{n_e}^{\rm tar}(t)$, the reference plasma $\bar{n_e}^{ref}(t)$ and the plasma superposed by ECH $\bar{n_e}(t)$. The profile of the enhanced particle flux $\Gamma_{\rm ECH}(\rho)$ is deduced from the continuous equation using the density decay $\partial n_e(\rho, t_0)/\partial t$ after the ECH is turned on($t = t_0$),

$$\Gamma_{\rm ECH}(\rho) = \frac{a}{\rho}\int_0^\rho \rho' \frac{\partial n_e(\rho', t_0)}{\partial t} {\rm d}\rho', \quad (1)$$

$$\frac{\partial n_e(\rho, t_0)}{\partial t} = \frac{\Delta \bar{n_e}(\infty)}{\tau_{\rm nl}} \frac{n_e(\rho, t_1) - n_e^{\rm tar}(\rho, t_1)}{\bar{n_e}(t_1) - \bar{n_e}^{\rm tar}(t_1)}. \quad (2)$$

Here, $n_e^{\rm tar}(\rho, t_1)$ and $n_e(\rho, t_1)$ are the electron density profiles measured with TS($t = t_1$) for the target plasma and that superposed by ECH, respectively. $\Delta \bar{n_e}(\infty)/\tau_{\rm nl}$ is given by the fitting of $\Delta \bar{n_e}(t)$[$\equiv \bar{n_e}(t) - \bar{n_e}^{\rm tar}(t)$] as $\Delta \bar{n_e}(\infty)$[$1 - \exp[-(t - t_0)/\tau_{\rm nl}]$]. Since the gas puffing rates are adjusted as same both for the target plasma and that superposed by ECH, the difference of the source term $\Delta S(\rho, t)$[$\equiv S(\rho, t) - S^{\rm tar}(\rho, t)$] is neglected. At $t = t_1$, H_α intensity for the plasma superposed by ECH increases

by about 20% of that for the target plasma due to the degradation of the particle confinement by ECH. The evaluated profiles $\Gamma_{ECH}(\rho)$ are shown in Fig.2(c) for the plasmas with P_{ECH}=85 and 140kW. The error bars in Fig.2(c) come from the fitted $\Delta\bar{n}_e(\infty)$ and τ_{ni}. Figure 2(c) shows also the profile of the neoclassical flux $\Gamma^{NC}(\rho)$ for the target plasma, which is estimated from the connection formula of neoclassical transport that covers the whole collisionality regime [Eqs.(6)-(11) in Ref.10] by using the fitting curves for $n_e(\rho)$, $T_e(\rho)$ and $T_i(\rho)$. For simplicity, we assume a single helicity model in the theoretical calculations. Both ions and electrons for the reference and the target plasma are in plateau regime in the whole plasma region. For the plasma superposed by ECH, although ions are in plateau regime, electrons are in the $1/\nu$ regime (electron collisionality $\nu_{*\,e}[=(qR/\varepsilon_h^{1.5}v_{th})\nu]>0.5$) at $\rho\gtrsim$0.6-0.9. Here, ν is the pitch angle scattering frequency by the collisions, q is a safty factor, ε_h is the helical ripple and v_{th} is a thermal velocity.

Figure 3(a) shows the observed radial electric field profiles for the reference plasma and that with P_{ECH}=140kW. The large positive electric field is observed near the plasma edge for the plasma with P_{ECH}=140kW($\sim$44V cm^{-1} at ρ=0.82). Figure 3(a) also shows the radial electric field profiles evaluated theoretically from an ambipolarity equation[25], $\Gamma_e^{NC} + \Gamma_{ECH} = \Gamma_i^{NC}$. Here, we assume that ECH enhances only electron particle flux, not ion particle flux. It is noted that the ambipolarity equation gives

the upper limit of the radial electric field on each magnetic surface. The profile of the calculated electric field is not in agreement with that of the observed electric field for the plasma with P_{ECH}=140kW. The calculated electric field is more positive at the plasma edge(ρ >0.8), and is more negative at the core region than the observed electric field. The ambipolarity equation may contain multiple solutions and causes the discontinuities in the electric field profile, because it is given on the each magnetic surface. If the transition of the radial electric field occurs in the outer region, the electric field diffuses into the inner region under the influence of the perpendicular viscosity. Therefore, the theoretically evaluated electric field should become more smooth radial profile such as that of the observed electric field by taking the diffusion process of the electric field into consideration. To explain the transition phenomena qualitatively, we restrict our results to the electric field at ρ=0.82. Figure 3(b) shows a dependence of the radial electric field on the enhanced flux Γ_{ECH} for various P_{ECH} at ρ=0.82. The transition of the radial electric field from a negative(the ion root) to a positive value(the electron root) is observed at the larger enhanced flux($\sim 4 \times 10^{15}\mathrm{cm}^{-2}\mathrm{s}^{-1}$). Although the enhanced flux becomes large when the plasma is heated with the higher P_{ECH}, it does not change much even though the higher P_{ECH} is injected after the transition occurs. Since the obtained density and temperature profiles are different in this power scan experiment, the neoclassical fluxes estimated from the profiles change a

little. The scattering of the theoretical predictions in Fig.3(b) is caused by the change of the neoclassical fluxes. The ion neoclassical flux strongly depends on the radial electric field E_r and has a peak at $E_r \simeq 0$ while the electron neoclassical flux has a weak dependence on the radial electric field. If the additional electron loss flux Γ_{ECH} is small, the ambipolarity constraint does not affect much the radial electric field. However, if Γ_{ECH} is increased and becomes large enough to have multiple solutions, the transition occurs.

Further technical improvement is required to show experimentally clear transition phenomena such that the electric field changes dramatically at a critical P_{ECH} during ramping up P_{ECH}. As for the theoretical model, we do not discuss the dependence of the enhanced flux Γ_{ECH} on the radial electric field. To understand the mechanism causing the enhanced flux is extremely important but it is the future work.

In conclusion, the transition of the radial electric field is observed by enhancing sufficiently the electron flux with the second harmonic ECH in CHS. The observed transition is qualitatively explained by the theoretical model based on the ambipolarity equation.

One of the authors(H.I) wishes to express his thank Dr. T. Watari for his encouragement and discussion. The authors would like to thank members of the torus experimental group for fruitful discussions and also to the technical staffs for the oper-

ation of ECH and NB systems. This work is partially supported by the Grant-in-Aid from the Ministry of Education.

[a]Present Address: Plasma Science Center, Nagoya University, Nagoya 464-01, Japan

[1] F. Wagner, G. Backer, K. Behringer, D. Campbell, A. Eberhagen *et al.*, Phys. Rev. Lett. **49**, 1408 (1982).

[2] R. J. Groebner, K. H. Burrel and R. P. Seraydarian, Phys. Rev. Let. **64**, 3015 (1990).

[3] K. Ida, S. Hidekuma, Y. Miura, T. Fujita, M. Mori *et al.*, Phys. Rev. Lett. **65**, 1364 (1990).

[4] S.-I. Itoh and K. Itoh, Phys. Rev. Lett. **60**, 2276 (1988)

[5] K. C. Shaing and E. C. Crume, Jr., Phys. Rev. Lett. **63**, 2369 (1989)

[6] H. Biglari, P. H. Diamond and P. W. Terry, Phys. Fluids **B2**, 1 (1990)

[7] A. B. Hassam, T. M. Antonsen, Jr., J. F. Drake and C. S. Liu, Phys. Rev. Lett. **66**, 309 (1991)

[8] F. L. Hinton, Phys. Fluids **B3**, 696 (1991)

[9] H. E. Mynick and W. N. G. Hitchon, Nucl. Fusion **23**, 1053 (1983).

[10] L. M. Kovrizhnykh, Nucl. Fusion **24**, 435 (1984).

[11] D. E. Hastings, W. A. Houlberg and K. C. Shaing, Nucl. Fusion **25**, 445 (1985).

[12] K. Kondo, H. Zushi, S. Nishimura, H. Kaneko, M. Sato *et al.*, Rev. Sci. Instrum. **59**,

1533 (1988).

[13] H. Wobig, H. Massberg, H. Renner, The WVII-A Team, the ECRH Group and the NI Group, in *Plasma Physics and Controlled Nuclear Fusion Reserch, 1986*, Kyoto(IAEA Vienna 1987) Vol.II p.369

[14] K. Matsuoka, S. Kubo, M. Hosokawa, Y. Takita, S. Okamura *et al.*, in *Plasma Physics and Controlled Nuclear Fusion Reserch, 1988*, Nice(IAEA Vienna 1989) Vol.II p.411.

[15] K. Ida, H. Yamada, H. Iguchi, S. Hidekuma, H. Sanuki, K. Yamazaki and the CHS Group, Phys. Fluids **B3**, 515 (1991); **B4**, 1360 (1992)

[16] H. Hsuan, K. Bol, N. Bowen, D. Boyd, A. Cavallo *et al.*, in *Heating in Toroidal Plasmas (Proc. 4th Int. Symp., Rome, 1984)*, Vol.2, International School of Plasma Physics, Varenna 809 (1984).

[17] F. Sardei, H. Ringler, A. Dodhy, G. Kühner, WVII-AS Group and ECRH Group, in *Proceedings of 17th EPS Conf. on Controlled Fusion and Plasma Heating, Amsterdam, 1990*, Vol.14B part II p.471.

[18] H. Zushi, M. Sato, O. Motojima, S. Sudo, T. Mutoh *et al.*, Nucl. Fusion **28**, 1801 (1988).

[19] S. Kubo, H. Idei, M. Hosokawa, Y. Takita, H. Iguchi *et al.*, in *Proceedings of International Conference on Plasma Physics, Innsbruck, 1992*, Vol.16C part.I p.513.

[20] K. Itoh, S.-I. Itoh, and A. Fukuyama, J. Phys. Soc. Japan **58**, 482 (1989).

[21] O. Kaneko, S. Kubo, K. Nishimura, T. Shoji, M. Hosokawa *et al.*, in *Plasma Physics and Controlled Nuclear Fusion Reserch, 1990*, Washington(IAEA Vienna 1991) Vol.II p.473.

[22] K. Ida and S. Hidekuma, Rev. Sci. Instrum. **60**, 876 (1989).

[23] K. Ida, H. Yamada, H. Iguchi, K. Itoh and CHS Group, Phys. Rev. Lett. **67**, 58 (1991)

[24] H. Yamada, K. Ida, H. Iguchi, S. Morita, O. Kaneko *et al.*, Nucl. Fusion **32**, 25 (1992).

[25] H. Sanuki, K. Itoh, K. Ida and S.-I. Itoh, J. Phys. Soc. Japan **60**, 3698 (1991).

Figure Captions

Fig.1 : Radial profiles of (a) electron density, (b) electron temperature, (c)ion temperature and (d)poloidal rotation velocity for the reference plasma and those with the injection power P_{ECH}=85 and 140kW. The electron density profile for the target plasma is also shown in (a).

Fig.2 : Time evolutions of (a) line-averaged electron densities of the target plasma, the reference plasma and that superposed by ECH, $\bar{n_e}^{tar}(t)$, $\bar{n_e}^{ref}(t)$ and $\bar{n_e}(t)$, and (b) the difference, $\Delta\bar{n_e}(t)[\equiv \bar{n_e}(t)-\bar{n_e}^{tar}(t)]$. (c) Radial profiles of enhanced fluxes Γ_{ECH} for the plasmas with the injection power P_{ECH}=85 and 140kW, and a neoclassical flux Γ^{NC} for the target plasma.

Fig.3 : (a) Radial electric field profiles for the reference plasma and that with the injection power P_{ECH}=140kW. Open and closed circles show observed radial electric fields. Broken and solid curves show calculated ones. (b) Radial electric fields E_r versus enhanced fluxes Γ_{ECH} at ρ=0.82 for the plasmas with various P_{ECH}. Closed circles show the observed E_r and hatched area represents the theoretical prediction.

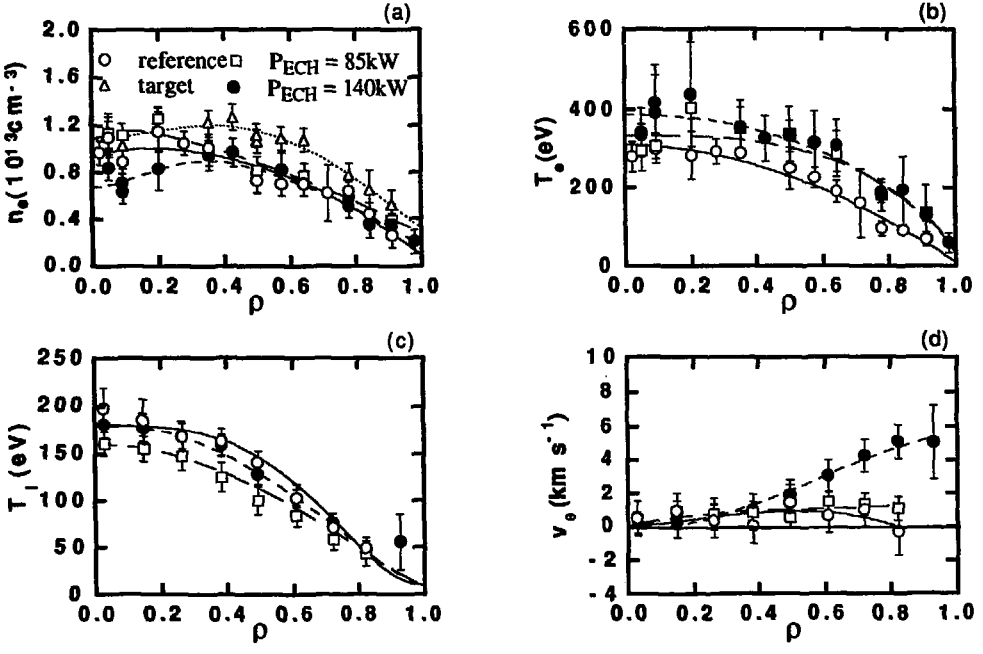
(a)
reference
target
P_{ECH} = 85kW
P_{ECH} = 140kW
n_e(10^{13}cm^{-3})
ρ
(b)
T_e(eV)
ρ
(c)
T_i (eV)
ρ
(d)
v_θ (km s^{-1})
ρ

Fig.1

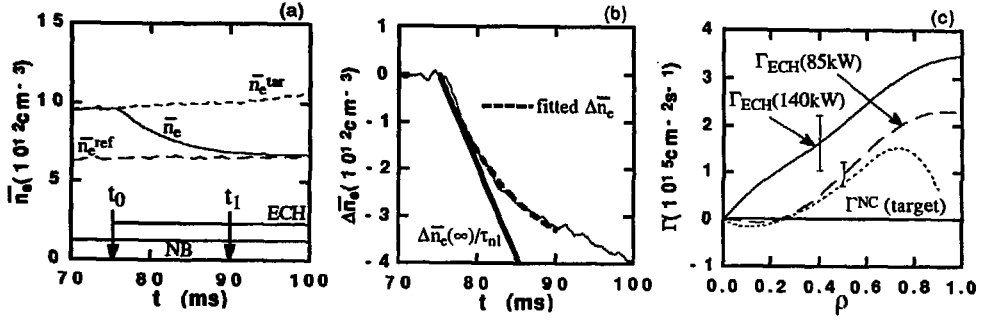
(a)
(b)
(c)
$\bar{n}_e^{tar}$
$\bar{n}_e$
$\bar{n}_e^{ref}$
t_0
t_1
ECH
NB
t (ms)
fitted $\Delta\bar{n}_e$
$\Delta\bar{n}_e(\infty)/\tau_{nl}$
Γ_{ECH}(85kW)
Γ_{ECH}(140kW)
Γ^{NC} (target)
ρ

Fig.2

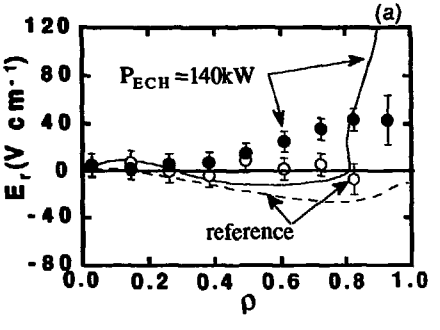
(a)
120
80
40
0
-40
-80
E_r(V cm^{-1})
P_{ECH}=140kW
reference
0.0
0.2
0.4
0.6
0.8
1.0
ρ

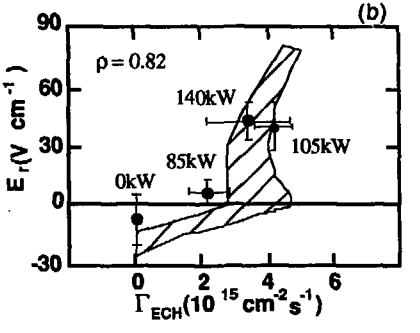
(b)
90
60
30
0
-30
E_r(V cm^{-1})
ρ = 0.82
140kW
105kW
85kW
0kW
0
2
4
6
Γ_{ECH}(10^{15}cm^{-2}s^{-1})

Fig.3

Recent Issues of NIFS Series

NIFS-183 S. Morimoto, M. Sato, H. Yamada, H. Ji, S. Okamura, S. Kubo, O. Motojima, M. Murakami, T. C. Jernigan, T. S. Bigelow, A. C. England, R. S. Isler, J. F. Lyon, C. H. Ma, D. A. Rasmussen, C. R. Schaich, J. B. Wilgen and J. L. Yarber, *Long Pulse Discharges Sustained by Second Harmonic Electron Cyclotron Heating Using a 35GH$_Z$ Gyrotron in the Advanced Toroidal Facility*; Sep. 1992

NIFS-184 S. Okamura, K. Hanatani, K. Nishimura, R. Akiyama, T. Amano, H. Arimoto, M. Fujiwara, M. Hosokawa, K. Ida, H. Idei, H. Iguchi, O. Kaneko, T. Kawamoto, S. Kubo, R. Kumazawa, K. Matsuoka, S. Morita, O. Motojima, T. Mutoh, N. Nakajima, N. Noda, M. Okamoto, T. Ozaki, A. Sagara, S. Sakakibara, H. Sanuki, T. Seki, T. Shoji, F. Shimbo, C. Takahashi, Y. Takeiri, Y. Takita, K. Toi, K. Tsumori, M. Ueda, T. Watari, H. Yamada and I. Yamada, *Heating Experiments Using Neutral Beams with Variable Injection Angle and ICRF Waves in CHS* ; Sep. 1992

NIFS-185 H. Yamada, S. Morita, K. Ida, S. Okamura, H. Iguchi, S. Sakakibara, K. Nishimura, R. Akiyama, H. Arimoto, M. Fujiwara, K. Hanatani, S. P. Hirshman, K. Ichiguchi, H. Idei, O. Kaneko, T. Kawamoto, S. Kubo, D. K. Lee, K. Matsuoka, O. Motojima, T. Ozaki, V. D. Pustovitov, A. Sagara, H. Sanuki, T. Shoji, C. Takahashi, Y. Takeiri, Y. Takita, S. Tanahashi, J. Todoroki, K. Toi, K. Tsumori, M. Ueda and I. Yamada, *MHD and Confinement Characteristics in the High-β Regime on the CHS Low-Aspect-Ratio Heliotron / Torsatron* ; Sep. 1992

NIFS-186 S. Morita, H. Yamada, H. Iguchi, K. Adati, R. Akiyama, H. Arimoto, M. Fujiwara, Y. Hamada, K. Ida, H. Idei, O. Kaneko, K. Kawahata, T. Kawamoto, S. Kubo, R. Kumazawa, K. Matsuoka, T. Morisaki, K. Nishimura, S. Okamura, T. Ozaki, T. Seki, M. Sakurai, S, Sakakibara, A. Sagara, C. Takahashi, Y. Takeiri, H. Takenaga, Y. Takita, K. Toi, K. Tsumori, K. Uchino, M. Ueda, T. Watari, I. Yamada, *A Role of Neutral Hydrogen in CHS Plasmas with Reheat and Collapse and Comparison with JIPP T-IIU Tokamak Plasmas* ; Sep. 1992

NIFS-187 K. Ioth, S.-I. Itoh, A. Fukuyama, M. Yagi and M. Azumi, *Model of the L-Mode Confinement in Tokamaks* ; Sep. 1992

NIFS-188 K. Itoh, A. Fukuyama and S.-I. Itoh, *Beta-Limiting Phenomena in High-Aspect-Ratio Toroidal Helical Plasmas*; Oct. 1992

NIFS-189 K. Itoh, S. -I. Itoh and A. Fukuyama, *Cross Field Ion Motion at Sawtooth Crash* ; Oct. 1992

NIFS-190 N. Noda, Y. Kubota, A. Sagara, N. Ohyabu, K. Akaishi, H. Ji, O. Motojima, M. Hashiba, I. Fujita, T. Hino, T. Yamashina, T. Matsuda, T. Sogabe, T. Matsumoto, K. Kuroda, S. Yamazaki, H. Ise, J. Adachi and T. Suzuki, *Design Study on Divertor Plates of Large Helical Device (LHD)* ; Oct. 1992

NIFS-191 Y. Kondoh, Y. Hosaka and K. Ishii, *Kernel Optimum Nearly-Analytical Discretization (KOND) Algorithm Applied to Parabolic and Hyperbolic Equations* : Oct. 1992

NIFS-192 K. Itoh, M. Yagi, S.-I. Itoh, A. Fukuyama and M. Azumi, *L-Mode Confinement Model Based on Transport-MHD Theory in Tokamaks* ; Oct. 1992

NIFS-193 T. Watari, *Review of Japanese Results on Heating and Current Drive* ; Oct. 1992

NIFS-194 Y. Kondoh, *Eigenfunction for Dissipative Dynamics Operator and Attractor of Dissipative Structure* ; Oct. 1992

NIFS-195 T. Watanabe, H. Oya, K. Watanabe and T. Sato, *Comprehensive Simulation Study on Local and Global Development of Auroral Arcs and Field-Aligned Potentials* ; Oct. 1992

NIFS-196 T. Mori, K. Akaishi, Y. Kubota, O. Motojima, M. Mushiaki, Y. Funato and Y. Hanaoka, *Pumping Experiment of Water on B and LaB_6 Films with Electron Beam Evaporator* ; Oct., 1992

NIFS-197 T. Kato and K. Masai, *X-ray Spectra from Hinotori Satellite and Suprathermal Electrons* ; Oct. 1992

NIFS-198 K. Toi, S. Okamura, H. Iguchi, H. Yamada, S. Morita, S. Sakakibara, K. Ida, K. Nishimura, K. Matsuoka, R. Akiyama, H. Arimoto, M. Fujiwara, M. Hosokawa, H. Idei, O. Kaneko, S. Kubo, A. Sagara, C. Takahashi, Y. Takeiri, Y. Takita, K. Tsumori, I. Yamada and H. Zushi, *Formation of H-mode Like Transport Barrier in the CHS Heliotron / Torsatron* ; Oct. 1992

NIFS-199 M. Tanaka, *A Kinetic Simulation of Low-Frequency Electromagnetic Phenomena in Inhomogeneous Plasmas of Three-Dimensions* ; Nov. 1992

NIFS-200 K. Itoh, S.-I. Itoh, H. Sanuki and A. Fukuyama, *Roles of Electric Field on Toroidal Magnetic Confinement*, Nov. 1992

NIFS-201 G. Gnudi and T. Hatori, *Hamiltonian for the Toroidal Helical Magnetic Field Lines in the Vacuum*; Nov. 1992

NIFS-202 K. Itoh, S.-I. Itoh and A. Fukuyama, *Physics of Transport Phenomena in Magnetic Confinement Plasmas*; Dec. 1992

NIFS-203 Y. Hamada, Y. Kawasumi, H. Iguchi, A. Fujisawa, Y. Abe and M. Takahashi, *Mesh Effect in a Parallel Plate Analyzer*; Dec. 1992

NIFS-204 T. Okada and H. Tazawa, *Two-Stream Instability for a Light Ion Beam -Plasma System with External Magnetic Field;* Dec. 1992

NIFS-205 M. Osakabe, S. Itoh, Y. Gotoh, M. Sasao and J. Fujita, *A Compact Neutron Counter Telescope with Thick Radiator (Cotetra) for Fusion Experiment*; Jan. 1993

NIFS-206 T. Yabe and F. Xiao, *Tracking Sharp Interface of Two Fluids by the CIP (Cubic-Interpolated Propagation) Scheme*, Jan. 1993

NIFS-207 A. Kageyama, K. Watanabe and T. Sato, *Simulation Study of MHD Dynamo : Convection in a Rotating Spherical Shell*; Feb. 1993

NIFS-208 M. Okamoto and S. Murakami, *Plasma Heating in Toroidal Systems*; Feb. 1993

NIFS-209 K. Masai, *Density Dependence of Line Intensities and Application to Plasma Diagnostics*; Feb. 1993

NIFS-210 K. Ohkubo, M. Hosokawa, S. Kubo, M. Sato, Y. Takita and T. Kuroda, *R&D of Transmission Lines for ECH System* ; Feb. 1993

NIFS-211 A. A. Shishkin, K. Y. Watanabe, K. Yamazaki, O. Motojima, D. L. Grekov, M. S. Smirnova and A. V. Zolotukhin, *Some Features of Particle Orbit Behavior in LHD Configurations*; Mar. 1993

NIFS-212 Y. Kondoh, Y. Hosaka and J.-L. Liang, *Demonstration for Novel Self-organization Theory by Three-Dimensional Magnetohydrodynamic Simulation*; Mar. 1993

NIFS-213 K. Itoh, H. Sanuki and S.-I. Itoh, *Thermal and Electric Oscillation Driven by Orbit Loss in Helical Systems*; Mar. 1993

NIFS-214 T. Yamagishi, *Effect of Continuous Eigenvalue Spectrum on Plasma Transport in Toroidal Systems*; Mar. 1993

NIFS-215 K. Ida, K. Itoh, S.-I.Itoh, Y. Miura, JFT-2M Group and A. Fukuyama, *Thickness of the Layer of Strong Radial Electric Field in JFT-2M H-mode Plasmas*; Apr. 1993

NIFS-216 M. Yagi, K. Itoh, S.-I. Itoh, A. Fukuyama and M. Azumi, *Analysis of*

Current Diffusive Ballooning Mode; Apr. 1993

NIFS-217 J. Guasp, K. Yamazaki and O. Motojima, *Particle Orbit Analysis for LHD Helical Axis Configurations* ; Apr. 1993

NIFS-218 T. Yabe, T. Ito and M. Okazaki, *Holography Machine HORN-1 for Computer-aided Retrieve of Virtual Three-dimensional Image* ; Apr. 1993

NIFS-219 K. Itoh, S.-I. Itoh, A. Fukuyama, M. Yagi and M. Azumi, *Self-sustained Turbulence and L-Mode Confinement in Toroidal Plasmas* ; Apr. 1993

NIFS-220 T. Watari, R. Kumazawa, T. Mutoh, T. Seki, K. Nishimura and F. Shimpo, *Applications of Non-resonant RF Forces to Improvement of Tokamak Reactor Performances Part I: Application of Ponderomotive Force* ; May 1993

NIFS-221 S.-I. Itoh, K. Itoh, and A. Fukuyama, *ELMy-H mode as Limit Cycle and Transient Responses of H-modes in Tokamaks* ; May 1993

NIFS-222 H. Hojo, M. Inutake, M. Ichimura, R. Katsumata and T. Watanabe, *Interchange Stability Criteria for Anisotropic Central-Cell Plasmas in the Tandem Mirror GAMMA 10* ; May 1993

NIFS-223 K. Itoh, S.-I. Itoh, M. Yagi, A. Fukuyama and M. Azumi, *Theory of Pseudo-Classical Confinement and Transmutation to L-Mode;* May 1993

NIFS-224 M. Tanaka, *HIDENEK: An Implicit Particle Simulation of Kinetic-MHD Phenomena in Three-Dimensional Plasmas;* May 1993

NIFS-225 H. Hojo and T. Hatori, *Bounce Resonance Heating and Transport in a Magnetic Mirror;* May 1993

NIFS-226 S.-I. Itoh, K. Itoh, A. Fukuyama, M. Yagi, *Theory of Anomalous Transport in H-Mode Plasmas;* May 1993

NIFS-227 T. Yamagishi, *Anomalous Cross Field Flux in CHS Torsatron*; May 1993

NIFS-228 Y. Ohkouchi, S. Sasaki, S. Takamura, T. Kato, *Effective Emission and Ionization Rate Coefficients of Atomic Carbons in Plasmas;* June 1993

NIFS-229 K. Itoh, M. Yagi, A. Fukuyama, S.-I. Itoh and M. Azumi, *Comment on 'A Mean Field Ohm's Law for Collisionless Plasmas;* June 1993